

# ABC Based Neural Network Method for Brain Tumor Identification from MRI and CT Images

Mitha Rachel Jose, J. Amar Pratap Singh



**Abstract:** According to the inconsistency and complication of tumors, MRI is a complicated method for categorizing brain tumor. Generally, the classification accuracy is enhanced by the help of pre-processing and feature extraction processes which are essential methods. In this document, we enhanced a brain tumor recognition process through ABC-ANN procedure. The anticipated procedure contains three segments such as Preprocessing, feature extraction and classification. Initially, the median filter and Histogram Equalization methods are used to augment the images. The second and third segments are FFT related attribute extraction and categorized by means of ABC related ANN method simultaneously.

**Keywords:** FFT-Fast Fourier Transform; ANN-Artificial Neural Network; ABC-Artificial Bee Colony algorithm; HE-Histogram Equalization.

## I. INTRODUCTION

Suppose, if a fault is origin hazard to appropriate analysis, then the exact recognition of medical image is a severe problem. Moreover, a plenty of data from medical examination are gathered for to verify the arithmetical consequence of the analysis [1, 2]. Also, medical examination is the process used for patient inspection, which take place by three dissimilar processes such as laboratory tests, bio-analyses (Electroencephalography (EEG), electrocardiography (EKG) etc.) and medical imaging analyses (MRI, BT, mammography etc.) (Strzelecki, 2013).

In medical image processing, efficient algorithms are essential to resolve compound geometric difficulties like segmentation, shape extraction, three-dimensional (3D) representation and listing of medical data. This distinctive geometric difficulty contains a suitable surface with a group of line data positions [3, 4, and 5]. Medical image segmentation is the foundation of medical image study. It is mainly used for pathology investigation, pathology handling and clinical analysis. So, it takes more computational time and high computational power necessities for large-scale data. In this document, the anticipated process contains mechanical multi-resolution image parameterization which is derived from texture depiction among specific association rules, united by means of image assessment among machine learning process.

Manuscript published on November 30, 2019.

\* Correspondence Author

Mitha Rachel Jose\*, Research Scholar, Noorul Islam University, Tamil Nadu, India.

J. Amar Pratap Singh, Professor and Director (Admin), Noorul Islam University, Tamil Nadu, India.

© The Authors. Published by Blue Eyes Intelligence Engineering and Sciences Publication (BEIESP). This is an open access article under the CC-BY-NC-ND license <http://creativecommons.org/licenses/by-nc-nd/4.0/>

Here, we employed dimensionality diminution procedure on casual attributes (feature selection), or merging them as extra useful in high-level attributes (feature construction) because this method gives a great quantity of low-level attributes (though extra useful than uncomplicated pixel intensity values), [6,7,8,9].

## II. LITERATURE REVIEW

Xinzheng Xu *et al* [10] have anticipated a process to combine multimodal medical images by means of the adaptive pulse-coupled neural networks (PCNN). It is optimized through the quantum-behaved particle swarm optimization (QPSO) algorithm. Additionally, the mutual information (MI), structural similarity (SSIM), image entropy (EN) are employed to evaluate the presentation of dissimilar process. K. Tsirikolias [11] have depicted a group of nonlinear L-filters which is derived from local data and known as Radius Filters (RFs). The fundamental scheme for the structure of RFs was the categorization of values in input signal as a sliding window. Here, RFs are uncomplicated, spontaneous and easy to execute in an exceptional signal arrangement, which supply insight and in-depth signal explanation for the appropriate filter design. Additionally, they indicate a simplification of the OS Filters, because it simply created from the RFs. A quantity of low level image processing functions like impulse noise elimination, speckle noise elimination, adjusting filtering, edge recognition in noisy images, image sharpening and image frequency disintegration.

Bobby G. Stuijzand *et al* [12] have anticipated a Medical image elucidation. It was shifting from 2D- to volumetric images. So, the alterations of cognitive and perceptual progressions are implicated. This is anticipated to concern the medical student cognitive load in learning image elucidation skill. Initially, they calculated human-computer communications for the period of two volumetric image elucidation processes. The concealed variable 'volumetric image information' was recognized from the data by the help of structural equation representation, which considerably envisage self-reported psychological attempt as a compute of cognitive load.

Anushikha Singh *et al* [13] have depicted a mechanical image processing which is based on the glaucoma analysis from the digital fundus image. Wavelet attribute removal is tracked by means of optimized genetic attribute choice united through numerous learning algorithms and diverse limitation surroundings. It is derived from attribute removal from the segmentation and blood vessel detached optic disc to develop the exactness of recognition.

## ABC Based Neural Network Method for Brain Tumor Identification from MRI and CT Images

In this analysis, the exactness of glaucoma recognition accomplished as high and glaucoma recognition from fundus image specify that it had enhanced exactness of categorization.

Lorenzo Putzu *et al* [14] have anticipated counting and categorization of blood cells. It is lead to the assessment and identification of an enormous quantity of diseases.

The investigation of white blood cells (WBCs) is used to recognize the acute lymphoblastic leukemia (ALL), a blood cancer as untreated. Presently, the morphological investigation of blood cells was carry out manually by means of expert machinist. On the other hand, this process contains several disadvantages such as slow investigation, irregular exactness, and dependences on the operator's proficiency. An illustration of mechanical systems that could examine and categorize blood cells had been described in the literature, and several systems are somewhat enhanced. A comprehensive and fully automated process for WBC

recognition and categorization with microscopic images was employed. In comparison, the nuclei was extra prominent than supplementary element, it segregate the complete leucocytes and divide the nucleus and cytoplasm. This method was essential to study every cell element in detail. In every cell element, dissimilar attributes like shape, color and texture are removed by means of method for surroundings pixel elimination. This attribute group was used to prepare dissimilar categorization representation for the detection of leukemia. Dissimilar categorization representations are permitted us to create that the support vector machine through a Gaussian radial origin kernel was the appropriate representation for the recognition of all, through superior exactness and compassion. Josefina Perlo *et al* [15] have proposed MR images of rubber profiles which is verified by means of a desktop MRI scanner. So, the insignificant spatial declaration of MR images was essentially lesser than visual process.

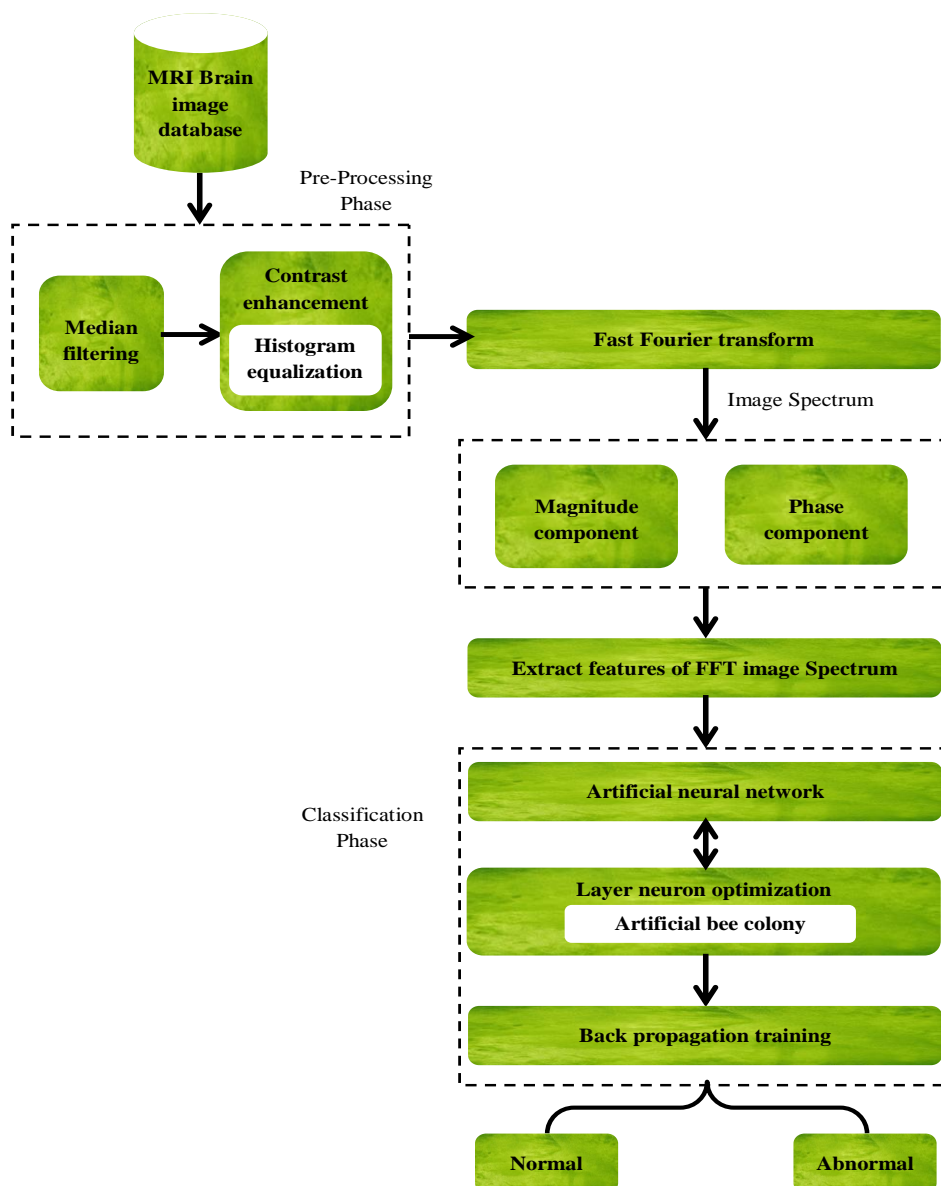


Fig. 1. Architecture Diagram of Proposed Method

### III. PROBLEM DEFINITION AND PROPOSED METHODOLOGY

The most general cancer areas are brain and central nervous system. According to the conversion of normal tissue areas into lesion areas by their intensity alteration, the computerized brain tumor segmentation procedure is really difficult one. Tumor arrangements are differ for each patient by their size, expansion, and localization. Therefore, we employed a great diversity of image modalities for mapping tumor-induced tissue alteration like MRI, MRSI etc. Each modality offer dissimilar kinds of genetic information like MRI image segmentation utilizing FFT curve analysis and k-space tumor recognition offers tumor classification. Besides, the previous recognition of brain tumor is simple through the Neural Network classifier. Therefore, these lack of solution and abovementioned problems are provoked me to perform investigation in this field (fig 1).

- To propose a procedure for the tumor recognition with FFT, curve analysis and neural network
- To estimate the procedure by the aid of dissimilar conventional MRI segmentation algorithms, and classification algorithms

Nowadays, Magnetic Resonance Imaging (MRI) is a significant device for medical analysis. In this document, we anticipated an effectual MRI image segmentation for tumor recognition by the help of FFT (Fast Fourier Transform), neural network among ABC optimization. At the start, the Median filter is pre-processing the input MRI image. And, the further pre-processing procedure Histogram Equalization is used to construct progression as suitable for supplementary processing by comparison. Afterward, the FFT contains the scale of the image. In this process, the attributes like mean, standard deviation, variance and correlation for both the segment and magnitude elements are take out from FFT. Moreover, the greatest and least values of the magnitude and segment elements are also obtained. At last, the Neural Network classifier is used to detect the brain tumor. The effectiveness of the medical image is enhanced by the ABC related Neural Network. The constant presentation is anticipated from the assessment process in diverse and practical situation.

#### A. Outline of Proposed ANN based Detection Approach:

The presented Brain Tumor Detection approach consists of three steps particularly,

- Pre-Processing
  - Median Filter
  - Histogram Equalization
- FFT based Feature Extraction
- ABC based Neural Network Classifier

##### a. Pre-Processing

The primary stage of medical imaging is pre-processing. Here, the pre-processing process is taken place by the aid of Median Filtering procedure.

##### 1. Median Filter:

In this process, the median filter is restoring the middle pixel by the help of median gray levels which decreases each pixel in the complete image. Here, we consider a filter as square windows of odd size because it is the common structure of median filter.

$$\hat{I}(m, n) = median\{I(m+t, n+v)\} \quad (1)$$

After this process, the image is proceeding by Histogram Equalization progression, which is used to expand the dissimilarity of the image.

##### 2. Equalization using Histogram Process:

Equalization is used to enhance the image contrast. Histogram equalization process expands the intensity values with the overall variety of values for to accomplish superior contrast. This process is more helpful when the image as close contrast values like the background and foreground are bright or dark at the identical time. The probability density is derived as

$$pdf_L(L_r) = \frac{f_r}{f} \quad (2)$$

$$g_i = \sum_{r=0}^i \frac{f_r}{f} = \sum_{r=0}^i pdf_L(L_r) \quad (3)$$

In this consequence, the expansion of contrast and the alteration of pixel intensity values are based on its local neighborhood. After this process, the images are subjected for feature removal procedure.

##### b. FFT based Feature Extraction

Fast Fourier Transform is a quick computation algorithm than the Discrete Fourier Transform (DFT) which is used to change the images from spatial field to Fourier or frequency field or vice versa. In the Fourier field, every position indicates the limited frequency in the spatial field image. Here, the computation of Fast Fourier Transform is used to remove the frequency field from the image attributes. The implementation of FFT to the image 'I(m, n)' is specified as:

$$FFT(I(m, n)) = F(x, y) = \sum_{m=0}^{P-1} \sum_{n=0}^{Q-1} I(m, n) \times \exp \left\{ -j2\pi \left( \frac{xm}{P} + \frac{yn}{Q} \right) \right\} \quad (4)$$

Where,  $m = n = 0, 1, \dots, 255$  indicates the dimension of image (i.e. the input images are resized as  $(256 \times 256)$ ) and  $(x, y)$  is the frequency elements in the image; moreover,  $I(m, n)$  and  $F(x, y)$  are the images which contains n spatial field and frequency field.

Also, the inverse of FFT can be derived as:

$$I(m, n) = \frac{1}{PQ} \sum_{x=0}^{P-1} \sum_{y=0}^{Q-1} F(x, y) \times \exp \left\{ j2\pi \left( \frac{xm}{P} + \frac{yn}{Q} \right) \right\} \quad (5)$$

The resultant image is separated as two segments (i.e. real and imaginary part) for the period of FFT computation. The real segment contains the magnitude and the other contains the stage. The magnitude division contains the information about the arithmetical arrangement of the spatial field image. And, the segment division contains the dissimilarity or the comparison of the image.

Moreover, the magnitude and phase of FFT can be computed as:

$$F(x, y) = |F(x, y)| \exp \{ j\eta(x, y) \} \quad (6)$$

The magnitude component  $|F(x, y)|$  can be again written as:

$$|F(x, y)| = \sqrt{F_{Real}^2(x, y) + F_{Img}^2(x, y)} \quad (7)$$

In above eqn,  $F_{Real}(x, y)$  and  $F_{Img}(x, y)$  denotes the real and imaginary parts of image.

Further, the phase component  $\eta(x, y)$  can be again written as:

$$\eta(x, y) = \arctan \left[ \frac{F_{Img}(x, y)}{F_{Real}(x, y)} \right] \quad (8)$$

Here, the appropriate attributes like mean, standard deviation, variance, correlation and the highest and least values of segment and magnitude are calculated for both the magnitude and phase elements. Here, the figure 2 illustrates about the FFT related features removal for the segment and magnitude elements. Therefore, the complete 12 attributes are removed for the FFT spectrum of each and every image.

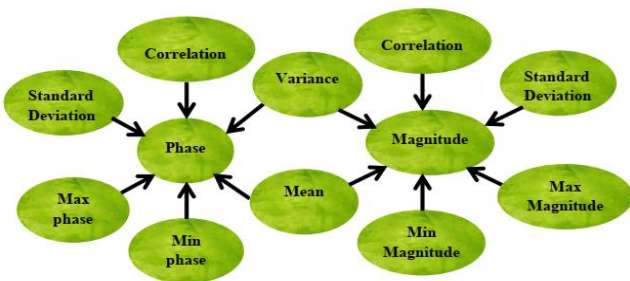


Fig. 2. FFT based features

The definitions and expressions of the feature extraction are as follows:

1. Mean ( $f_1$ ):

$$f_1 = \left( \frac{1}{PQ} \right) \sum_{x=1}^P \sum_{y=1}^Q |F(x, y)| \quad (9)$$

2. Variance ( $f_2$ ):

$$f_2 = \frac{1}{(P-1)(Q-1)} \sum_{x=1}^P \sum_{y=1}^Q (|F(x, y)| - f_1)^2 \quad (10)$$

3. Standard Deviation ( $f_3$ ): The standard deviation is like the average deviation, except the averaging is made by power rather than magnitude.

$$f_3 = \sqrt{\frac{1}{(P-1)(Q-1)} \sum_{x=1}^P \sum_{y=1}^Q (|F(x, y)| - f_1)^2} \quad (11)$$

4. Correlation ( $f_4$ ): Correlation is the expression which indicates the connection among pixels and its adjacent pixels. The correlation is specified in below equation,

$$f_4 = \left( \frac{1}{(P-1)(Q-1)} \right) \left( \frac{1}{f_3 \times f_3'} \right) \sum_{z=1}^Z \sum_{w=1}^W (|F(x, y)| - f_1) (|F'(x, y)| - f_1') \quad (12)$$

Where,  $|F'(x, y)|$  is the adjacent magnitude component of  $|F(x, y)|$ ;  $f_1'$  and  $f_3'$  are the mean and standard deviation of  $|F'(x, y)|$ .

5. Maximum Phase ( $f_5$ ): It is the peak value of phase of the image

6. Minimum Phase ( $f_6$ ): It is the least value of phase of the image

7. Maximum Magnitude ( $f_7$ ): It is the peak value of amplitude of the image

8. Minimum Magnitude ( $f_8$ ): It is the least value of amplitude of the image

Suppose, if the attribute removal progression is terminated, then the removed attributes are indicating the distinctive classes of the images. The categorization of standard and nonstandard images is prepared by means of ABC related ANN classifier.

c. ABC based Artificial neural network

The ANN is to provide effectual methods for data preprocessing, collection of structural design and preparation for the network. According to the unsystematic quantity of hidden nodes, it may create the difficulty of Overfitting and Underfitting. Therefore, the foremost difficulty of ANN is to choose the quantity of hidden nodes. Here, we established ABC optimization algorithm for to detect the finest quantity of hidden nodes with the artificial neural network for to develop the preparation presentation. The benefit of anticipated process is to calculate the quantity of hidden nodes by precise results. In anticipated process, the quantity of hidden nodes are not predefined but engendered in the preparation time.

The arrangement of ANN is specified in the beneath figure 3.

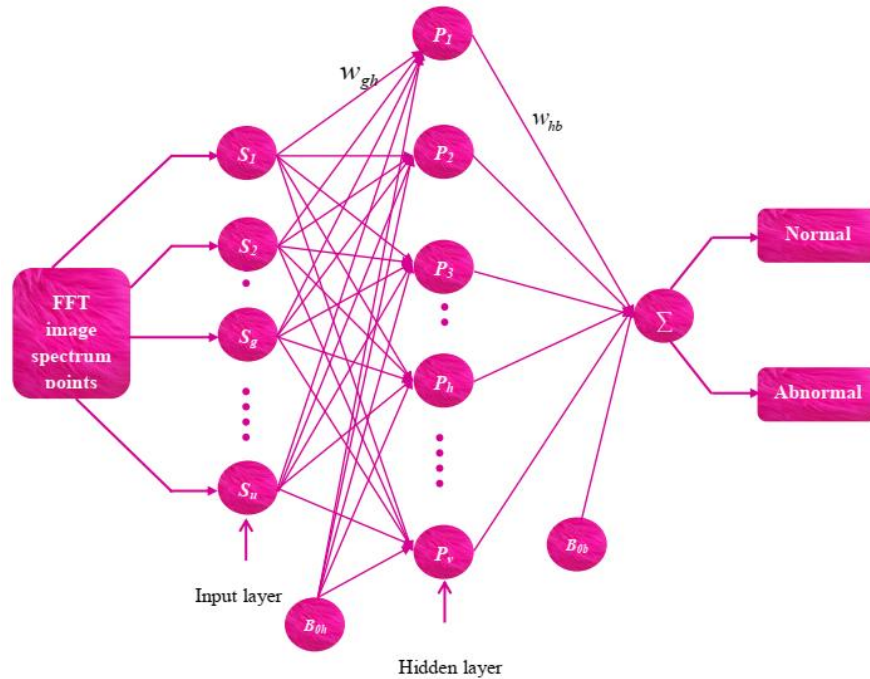


Fig. 3. Structure of ANN

i. Layer Neuron Optimization by ABC:

ABC algorithm encompasses three following phases such as,

- ❖ Employee Bee Phase
- ❖ Onlooker Bee Phase
- ❖ Scout Bee Phase

Initialization:

Initially, the populace of group is created randomly. Each consequence  $Z_w = \{z_{w,1}, z_{w,2}, \dots, z_{w,X}\}$  is a  $X$ -dimensional vector where  $X$  indicates the quantity of optimization limitation. According to the quantity of hidden layers and its neurons, the quantity of optimization limitation is diverging.

In each explanation  $Z_w = \{z_{w,1}, z_{w,2}, \dots, z_{w,X}\}$ , the initial expression indicates the quantity of chosen hidden layer and the residual expression provides the calculation of neurons essential to be preferred at every layer.

Fitness Evaluation:

Here, the fitness is anticipated by the food resource in the existing populace through the network structural design (i.e. the number of hidden layer and neuron composition). The evaluation of fitness is specified in below equation:

$$fitness = \max(Accuracy) \tag{13}$$

Where,

$$Accuracy = \frac{True\ Positive + True\ Negative}{True\ positiveP + True\ Negative + False\ Positive + False\ Negative} \tag{14}$$

The Accuracy value is used to find out the presentation of categorization. Therefore, the high accuracy value is

indicated as the intention task.

Employee Bee Phase:

In the employee bee segment, the food resources are reformed from the adjacent. The innovative explanation at ' $l^{th}$ ' location is established by means of beneath equation,

$$E_{wl} = z_{wl} + \beta_{wl}(Z_{wl} - Z_{kl}) \tag{15}$$

Where,  $\beta_{wl}(z_{wl} - z_{kl})$  is recognized as the dimension of step;  $\beta_{wl}$  is normally engendered among  $[-1, 1]$ ;  $Z_k$  is an arbitrarily preferred explanation (but  $w \neq k$ ), ' $k$ ' is the arbitrarily preferred dimension catalog from dimension  $(1, 2, \dots, X)$ . Moreover, the fitness is anticipated by the premature populace and the present created consequences. According to the fitness values, the consequences are alternated by means of the optimum consequence.

Onlooker Bee Phase:

In the onlooker bee phase, the food source is selected by the option. The onlooker bee selects the optimum food source which was obtained by means of the employee bee phase.

Probability Estimation:

The probability of selection will be made by the following equation

$$P(select) = \frac{fitness_w}{\sum_{l=1}^X fitness_l} \quad (16)$$

Here, the  $w^{th}$  explanation is preferred by the accomplishment of possibility value. Suppose, if the explanation is not accomplishing the possibility value, then the employee bee alter the location. In this process, whether it is good, the innovative explanation is modernized. If not, it is neglected. Suppose, if a location is not enhanced within three experimental calculation, then the scout bee segment is instigated. Here, the innovative explanations are engendered for the neglected ones.

**Scout Bee Phase:**

In the scout bee segment, the searching of innovative food source is organized for the ignored food source.

New solution will be generated for the scout bee phase is specified as,

$$S_{wl} = LB_l + (UB_l - LB_l)Rand(0,1) \quad (17)$$

Where,  $LB_l$ ,  $UB_l$  are the Minimum and Maximum limit of the search scope.

In the expansion segment, the scout bee is eliminating short fittest food possessions from the food source which is preferred at the employee bee segment.

**Updating:**

According to the fitness a value, the consequence of food source is modernized in anticipation of the optimum consequence is accomplished.

**Termination:**

Suppose, if maximum quantity of iteration is accomplished and then the process is concluded. Here, the finest network structural design is attained by consequences. The preparation of data is made by means of the network arrangement. Finally, the network is optimized by preparation of back propagation algorithm.

**ii. Neural Network: Back- Propagation Approach:**

Back propagation works on the basis on the following steps as;

**Stage 1:** Initialize the primary value of each interconnection weight among input to hidden and hidden to output layers as diminutive as unsystematic digit.

**Stage 2:** Establish the knowledge illustration pair and

activate  $S_u$

$$S_u = \begin{bmatrix} f_1^1, f_2^1, \dots, f_{12}^1 \\ f_1^2, f_2^2, \dots, f_{12}^2 \\ \vdots \\ f_1^t, f_2^t, \dots, f_{12}^t \end{bmatrix} \quad (18)$$

Where,  $f_1^1, f_2^1, \dots, f_{12}^1$  defines the features of sample image.

**Stage 3:** The computation of output layer is as follows

$$A_{(b)}^{NN(out)} = B_{0b} + \sum_{h=1}^v w_{hb} P_{(h)}^{NN} \quad (19)$$

Where,  $P_{(h)}^{NN} = \frac{1}{1 + \exp\left(-\sum_{g=1}^u w_{gh} S_{(g)} + B_{0h}\right)}$  (20)

**Stage 4:** Compute training error ( $\chi_{(b)}^{BP}$ )

$$\chi_{(b)}^{BP} = A_{(b)}^{NN(desired)} - A_{(b)}^{NN(out)} \quad (21)$$

Where,  $A_{(b)}^{NN(desired)}$  is the target label of the brain images?

**Stage 5:** Accurate weights for the subsequent iteration ( $w(i+1)$ ) is derived from the back propagation fault ( $\chi_{(b)}^{BP}$ ) and the weights of the existing iteration is ( $w(i)$ ).

$$w_{gh}(i+1) = w_{gh}(i) + \zeta \chi_{(b)}^{BP} \quad (22)$$

**Stage 6:** In this step, verify the outputs as whether congregate the exactness requirement in the preparation of illustration or conclude preparation progression.

**IV. EXPERIMENTAL ANALYSIS AND EVALUATION**

Here 39 MRI images and 18 CT images are obtained. Here, we brought 15 normal and 24 abnormal images in MRI and 11 normal and 7 abnormal images in CT scan. This acquired data was pre-processed, analyzed and classified for brain tumor detection in patients. In this experiment, the abnormal brain tumor image is identified by the help of FFT and ANN which is implemented in Matlab. Therefore, the projected ABC-ANN technique with MRI and CT images are exposed in figures 4 and 5.

The assessment of brain tumor detection is obtained from MRI and CT images which are shown in Figures 6 and 7



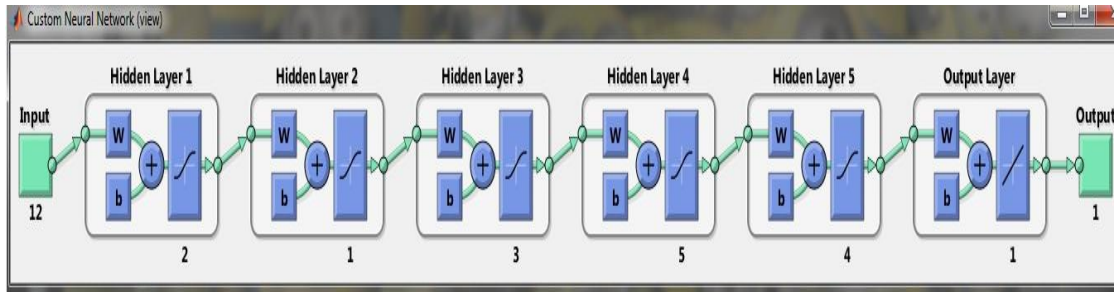


Fig. 4. Structure of ANN attained for MRI images

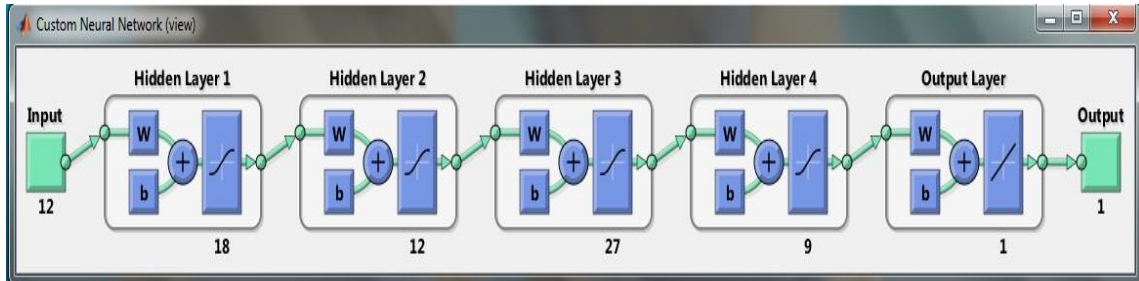


Fig. 5. Structure of ANN attained for CT images

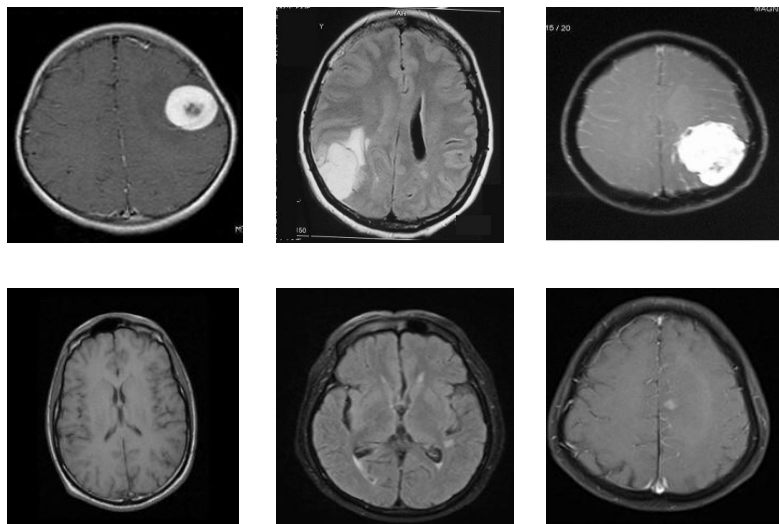


Fig. 6. Samples obtained from MRI images

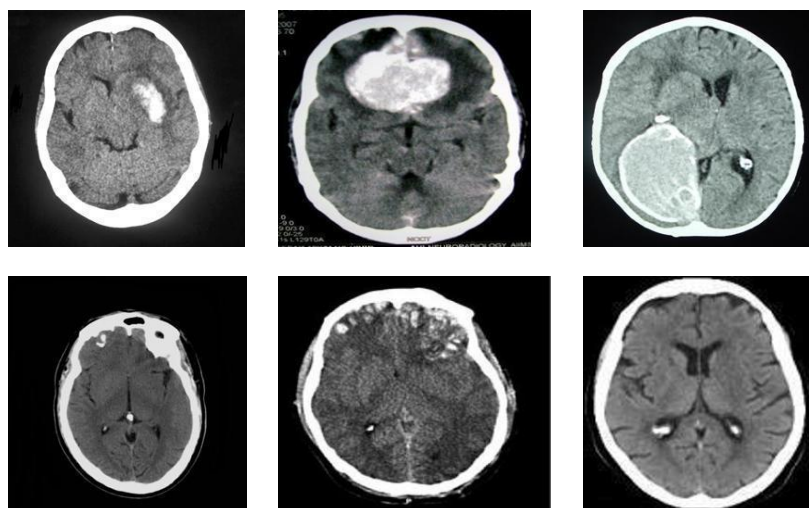


Fig. 7. Samples obtained from CT images

**A. Performance analysis**

From the MRI image, the training set contains 27 (normal-10 and abnormal-17) images and testing contains 12(normal-5 and abnormal-7). From CT image, the training set contains 12(normal-8 and abnormal-4) and testing set 6 (normal-3 and abnormal-3) which taken for the proposed ABC based Neural Network classification method. The Sensitivity, Specificity, Accuracy and False Acceptance Rate (FAR) ranges for MRI and CT images which are tabulated in the below (Table 1 to Table 8).

**Table 1: Sensitivity, Specificity, Accuracy and False Acceptance Rate for MRI Images (Training set 70 and Testing set 30)**

METRICS	ABC-ANN	PSO-ANN	GA-ANN	ANN
SENSITIVITY	1	0.4	0.4	0.6
SPECIFICITY	0.857143	1	0.857143	0.714286
ACCURACY	0.916667	0.75	0.666667	0.666667
FAR	0.142857	0	0.142857	0.285714

**Table 2: Sensitivity, Specificity, Accuracy and False Acceptance Rate for CT images (Training set 70 and Testing set 30)**

METRICS	ABC-ANN	PSO-ANN	GA-ANN	ANN
SENSITIVITY	0.666667	0	0.333333	0.666667
SPECIFICITY	1	1	0.666667	0.666667
ACCURACY	0.833333	0.6	0.5	0.666667
FAR	0	0	0.333333	0.333333

**Table 3: Sensitivity, Specificity, Accuracy and False Acceptance Rate values of MRI images. (80 training and 20 testing sets)**

METRICS	ABC-ANN	PSO-ANN	GA-ANN	ANN
SENSITIVITY	0.8	0.8	1	1
SPECIFICITY	1	0.666667	0	0.333333
ACCURACY	0.875	0.75	0.625	0.75
FAR	0	0.333333	1	0.666667

**Table 4: Sensitivity, Specificity, Accuracy and False Acceptance Rate values of CT images. (80 training and 20 testing sets)**

METRICS	ABC-ANN	PSO-ANN	GA-ANN	ANN
SENSITIVITY	1	0.5	1	1
SPECIFICITY	0.5	0.5	0	0
ACCURACY	0.75	0.5	0.5	0.5
FAR	0.5	0.5	1	1

**Table 5: Sensitivity, Specificity, Accuracy and False Acceptance Rate values of MRI images. (60 training and 40 testing sets)**

METRICS	ABC-ANN	PSO-ANN	GA-ANN	ANN
SENSITIVITY	0.75	0.5	1	0.75
SPECIFICITY	0.833333	0.916667	0.25	0.666667
ACCURACY	0.8125	0.8125	0.4375	0.6875
FAR	0.166667	0.083333	0.75	0.333333

**Table 6: Sensitivity, Specificity, Accuracy and False Acceptance Rate values of CT images. (60 training and 40 testing sets)**

METRICS	ABC-ANN	PSO-ANN	GA-ANN	ANN
SENSITIVITY	1	0.8	0.8	0.25
SPECIFICITY	0	0	0	0.5
ACCURACY	0.714286	0.666667	0.571429	0.333333
FAR	1	1	1	0.5

**Table 7: Sensitivity, Specificity, Accuracy and False Acceptance Rate values of MRI images. (50 training and 50 testing sets)**

METRICS	ABC-ANN	PSO-ANN	GA-ANN	ANN
SENSITIVITY	0.8	0.6	1	1
SPECIFICITY	0.857143	0.928571	0.357143	0.642857
ACCURACY	0.842105	0.842105	0.526316	0.736842
FAR	0.142857	0.071429	0.642857	0.357143

**Table 8: Sensitivity, Specificity, Accuracy and False Acceptance Rate values of CT images. (50 training and 50 testing sets)**

METRICS	ABC-ANN	PSO-ANN	GA-ANN	ANN
SENSITIVITY	1	1	1	1
SPECIFICITY	0.4	0.2	0	0.2
ACCURACY	0.666667	0.5	0.5	0.555556
FAR	0.6	0.8	1	0.8

In the case of Specificity, the existing PSO-ANN technique is 100% than further techniques for MRI images and 100% for ABC-ANN and PSO-ANN in CT images.

While analyzing classification accuracy values, the proposed ABC-ANN technique is obtained 87% accurate in MRI and CT images when compared with other algorithms.

When analyzing the False Acceptance Rate, the existing method of PSO-ANN is obtained almost 100% and 85% for remaining techniques in MRI images. In CT image, the ABC-ANN and PSO-ANN technique are obtained 100% than any other techniques.

Finally, the Comparison Plot for Proposed and existing techniques in both MRI and CT images were specified in figure 8 and 9.

Therefore it is clearly noted that the performance outcomes of the proposed strategy ABC-ANN is better in terms of sensitivity, specificity, accuracy, false acceptance rate measures than the existing methods of PSO-ANN, GA-ANN and ANN.

**V. CONCLUSION**

In this document, we anticipated an effectual process for

brain tumor categorization by means of Artificial Bee Colony related Artificial Neural Network method. The presentation of anticipated ABC related ANN procedure is contrasted by means of the obtainable process. Additionally, the measurements like False Acceptance Rate, False Rejection Rate, Precision, Recall, and F-measure are evaluated for the anticipated and obtainable categorization procedure which is used to examine the categorization presentation. From the obtained consequences, we can terminate the anticipated process is capable of identifying the tumor division in both the MRI and CT image.

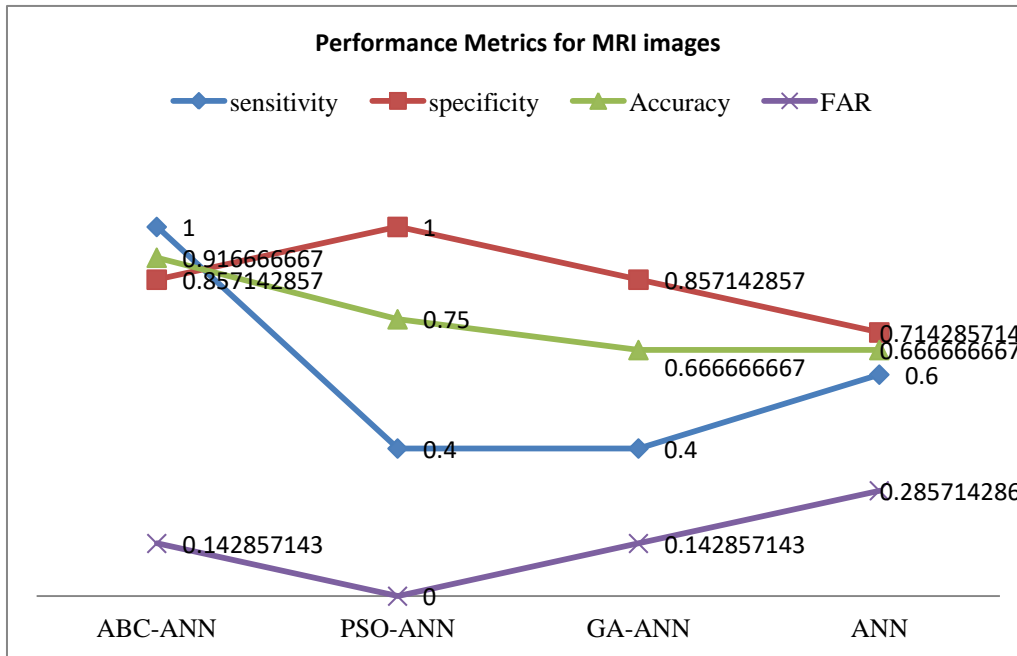


Figure 8: Comparison plot for proposed vs. existing technique for MRI images

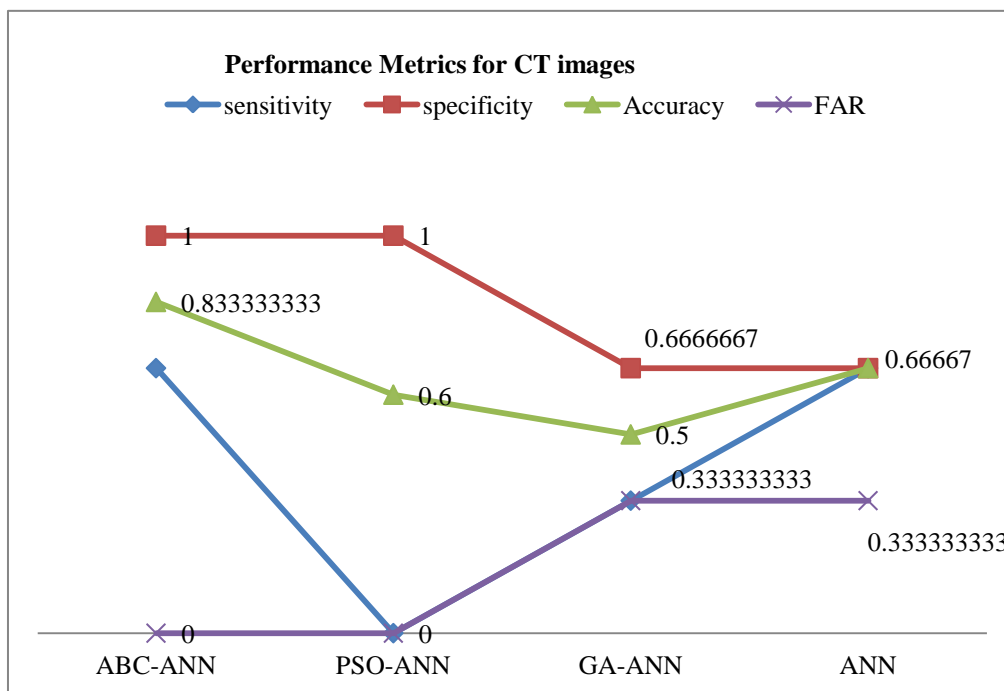


Figure 9: Comparison plot for proposed vs. existing technique for CT images.

REFERENCES

1. Oliver Reiche, KonradHäublein, Marc Reichenbach, Moritz Schmid, Frank Hannig, JürgenTeich and Dietmar Fey, "Synthesis and optimization of image processing accelerators using domain knowledge", Journal of Systems Architecture, vol. 61, no. 10, 2015, pp. 646-658.
2. Anders Eklund, Paul Dufort, Daniel Forsberg and Stephen M. LaConte, "Medical image processing on the GPU – Past, present and future", Medical Image Analysis, vol. 17, no. 8, 2013, pp. 1073-1094..
3. Oliver Reiche, KonradHäublein, Marc Reichenbach, Moritz Schmid, Frank Hannig,JürgenTeich and Dietmar Fey, "Synthesis and optimization of image processing accelerators using domain knowledge", Journal of Systems Architecture, vol. 61, no. 10, 2015, pp. 646-658.
4. Jie Tian, Jian Xue,Yakang Dai, Jian Chen and Jian Zheng, A Novel Software Platform for Medical Image Processing and Analyzing, IEEE Transactions on Information Technology in Biomedicine, vol. 12, no. 6, 2008, pp. 800-812.
5. A. Świetlicka, "Trained stochastic model of biological neural network used in image processing task", Applied Mathematics and Computation, vol. 267, 2015, pp. 716-726.
6. Cuma Son gurand Mehmet Top, "Regional clustering of medical imaging technologies", Computers in Human Behavior, vol. 61, 2016, pp. 333-343.
7. Luka Sajn and MatjaKukar, "Image processing and machine learning for fully automated probabilistic evaluation of medical images", Computer Methods and Programs in Biomedicine, vol. 104, no. 3, 2011, pp. e75-e86.
8. Fabian Rengier, Matthias F. Häfnerb, Roland Unterhinninghofenc, Ralph Nawrotzkid, Joachim Kirsch, Hans-Ulrich Kauczor and Frederik L. Giesel, "Integration of interactive three-dimensional image post-processing software into undergraduate radiology education effectively improves diagnostic skills and visual-spatial ability", European Journal of Radiology, vol. 82, no. 8, 2013, pp. 1366-1371.
9. Fan Zhao, Jian Zhao, Wenda Zhao, Feng Qu, Long Sui, "Local region statistics combining multi-parameter intensity fitting module for medical image segmentation with intensity inhomogeneity and complex composition", Optics & Laser Technology, vol. 82, 2016, pp. 17-27.
10. XinzhengXu, Dong Shan, Guanying Wang and Xiangying Jiang, "Multimodal medical image fusion using PCNN optimized by the QPSO algorithm", Applied Soft Computing, vol. 46, 2016, pp. 588-595.
11. K. Tsirikolias, "Low level image processing and analysis using radius filters", Digital Signal Processing, vol. 50, 2016, pp. 72-83.
12. Bobby G. Stuijtzand, Marieke F. van der Schaaf, Femke C. Kirschner,Cecile J. Ravesloot, Anouk van der Gijp, Koen L. Vincken, "Medical students' cognitive load in volumetric image interpretation: Insights from human-computer interaction and eye movements", Computers in Human Behavior, vol. 62, 2016, pp. 394-403.
13. Anushikha Singh, Malay Kishore Duttaa, M. ParthaSarathi,VaclavUherandRadimBurget, "Image processing based automatic diagnosis of glaucoma using wavelet features of segmented optic disc from fundus image", Computer Methods and Programs in Biomedicine, vol. 124, 2016, pp. 108-120.
14. Lorenzo Putzu, Giovanni Caocci and Cecilia Di Ruberto, "Leucocyte classification for leukaemia detection using image processing techniques", Artificial Intelligence in Medicine, vol. 62, no. 3, 2014, pp. 179-191.
15. Josefina Perlo, ChristophMülder, Ernesto Danieli, Christian Hopmann,BernhardBlümich, Federico Casanov, "Digital processing of images of extruded rubber profiles for process control MRI", Measurement, vol. 82, 2016, pp. 466-475.